

LITHOLOGICAL DISCRIMINATION OF SUN-FACING AND SHADOWED PORTIONS OF ARAVALLI REGION

Nilanchal Patel* and K. K. Rampal**

* Department of Civil Engineering, Indian Institute of Technology, Delhi, Hauz Khas, New Delhi-110 016, India

** Indian Institute of Remote Sensing, 4 Kalidas Road, Dehradun-248 001, India

ABSTRACT

Surface illumination in the mountainous terrains is characterized differently on the sun-facing and shadowed portions of the geologic units. This causes misclassification of the litho-units using satellite remotely sensed data. In the present paper, an effort has been made to use Landsat thematic mapper data for the classification of the different litho-units of the Aravalli mountains of Rajasthan State (India) by applying supervised maximum likelihood classifier. The various litho-units of the Aravalli region have been classified considering the sun-facing and shadowed portions of each unit as different classes based on ground truth data. A geological map prepared from the digital image is found to compare closely with the published geological map.

INTRODUCTION

Lithological discrimination constitutes one of the most important aspects of geologic remote sensing. Various statistical methods have been applied successfully to carry out lithological discrimination in geological terrains characterized by even topography /1-3/. In such terrains, owing to the prevalence of similar illumination conditions, the spectral characteristics of different litho-units remains unaffected. In contrast, there occurs significant brightness variation in the sun-facing and shadowed portions of the litho-units in the mountainous terrains. As a result, the spectral characteristics of the litho-units tend to vary considerably in the illuminated (sun-facing) and shadowed portions of their exposures. This causes misclassification of the litho-units in the digital classification of the remotely sensed data. Lithological discrimination in the mountainous terrains can, however, be carried out effectively by considering the sun-facing and shadowed portions of each litho-unit as different classes in the statistical classification of digital data.

In the present paper, an attempt has been made to classify different litho-units in a 512x512 subscene of Landsat-5 TM scene (path 148-row 043) constituting a part of the Aravalli mountains in Rajasthan state (India). In order to accomplish the task, we have used supervised maximum likelihood classifier assuming equal a-priori probability of each class. The major rock types present in the study area are granites, gneisses, phyllites, schists, quartzites and impure limestones as shown in the geological map published by the Geological Survey of India /4-5/ (Figure 1).

METHODOLOGY

Maximum likelihood classifier necessitates extraction of training data sets of different classes to be used in the classifier. In the present study, we have used all the spectral bands of TM data excluding the thermal band. The analysis has been carried out using three litho-units namely granites, phyllites and quartzites since only they could be identified on the various FCCs. In order to account for the brightness variation of the granitic and quartzitic rocks, the illuminated and shadowed portions of each of them have been considered as different classes based on ground truth data. Similarly, in order to reduce the effect of vegetation, two classes of vegetation have been selected for classification such as vegetation-1 and vegetation-2 representing the forested class and cultivated area respectively.

In order to evaluate the spectral separability between different classes, the training pixels of the classes were first classified. The result of this classification is

presented in form of a contingency table or confusion matrix in Table 1. The table shows the actual categories in rows and the predicted categories in columns where the actual categories are the ones already identified in the FCCs and the predicted categories represent the categories chosen by the analyst. The objective is to classify the training pixels of the actual categories as one or more predicted categories on the basis of their spectral similarity determined by the maximum likelihood classifier. The diagonal elements of this table represent the number of training pixels of each category correctly classified and the off-diagonal elements represent the number of incorrectly classified pixels of each actual category as the various predicted categories. The numbers of correctly classified pixels and the incorrectly classified pixels in the confusion matrix can be expressed in percentages as shown in Table 2. In the next step, the digital data of the entire subscene were classified in order to generate a thematic image as shown in Figure 2.

RESULTS AND DISCUSSIONS

Analysis of the contingency tables (Tables 1&2) reveals that no class was classified upto 100 percent accuracy. The individual rock type accuracies ranged from 56.8 percent for quartzite-2 to 90 percent accuracy for granite-2. Overall classification accuracy was 81.96 percent. 5242 pixels were correctly classified out of 6396 pixels sampled. Likewise, out of 6396 pixels sampled, 340 pixels (i.e. 5.32 percent) were unclassified, that is, they did not belong to any predicted class. Among the five predicted classes of rock types chosen, granite-2 was found to be the most misclassified class with the total number of training samples of all the actual categories misclassified as granite-2 being the largest, that is, 36.3 percent while the quartzite-2 proved to be the least misclassified class (6.85 percent). The contingency table (Table 1) also shows that with the exception of the water class, the cultivated cover class (class 2) was found to be the most dominantly represented class in the classified image since it is represented by 245.9 percent of its actual number of training pixels sampled. These observations indicate that most of the rock types show greater spectral affinity towards vegetation-2 (class 2) in comparison to vegetation-1 (class 1).

Further analysis of the contingency table (Table 2) reveals that out of the ten rock pairs possible, seven rock pairs exhibit distinct spectral separation of the rocks; these are namely quartzite-1 - quartzite-2, granite-1 - granite-2, phyllites - quartzite-2, phyllites - granite-1, phyllites - granite-2, quartzite-1, granite-1, and quartzite-1, granite-2. On the other hand, quartzite-2 misclassified as granite-2 to an extent of 23.3 percent while granite-2 misclassified as quartzite-2 by only 7.6 percent. This observation indicates that quartzite-2 has greater spectral affinity towards granite-2 in comparison to what granite-2 shows towards quartzite-2. Likewise, the phyllites and quartzite-1 show a mutual misclassification of 6.8 to 6.9 percent. The third pair showing misclassification is granite-1 and quartzite-2. Granite-1 misclassified as quartzite-2 by 4.6 percent while quartzite-2 misclassified as granite-1 by 2.6 percent.

Examination of the digital thematic image (Figure 2) reveals that the illuminated parts of the quartzitic terrain (quartzite-1) sharply demarcate from the non-illuminated parts (quartzite-2) on the basis of the colour difference. The illuminated parts of the quartzites show occasional presence of spectral signature of the illuminated parts of the granites (granite-1) but the shadowed parts of the quartzites is marked frequently by the presence of spectral signatures of the phyllites and granite-2. The illuminated parts of the granitic rocks are conspicuous by their dark brown signature and completely demarcate from their non-illuminated parts showing yellow colour. The granitic rocks, neither in their illuminated parts nor in the shadowed parts, exhibit presence of spectral signature of any other rock type. These observations are, in fact, consistent with the classification accuracies of the quartzites and the granites shown in the confusion matrix (Table 2). The phyllitic rocks can be distinguished from the other rock types on the basis of their even topography and greenish colour. The terrain comprising the phyllites and schists is also marked by the presence of spectral signatures closely resembling the granite-1 (illuminated), which is indicative of the presence of a fourth litho-unit.

Comparison of the digital thematic image and the published geological map (Figure 1) reveals that there is no sharp demarcation of different litho-units on the digital image vis-a-vis their dispositions in the published map. The similar spectral signatures of the Eripura granites and gneisses, and the biotitic limestones and the calc gneisses may be attributed to their identical constituent minerals and moreover, to the confusing influence of vegetation cover developed on them. Likewise, the intermixing of the phyllites and impure limestones with the calc schists may be explained by the same factors. Nevertheless, the contacts between the various geologic units can be located approximately on the thematic image which are shown in a lithological map prepared from the thematic image (Figure 3). Obviously, the illuminated and shadowed portions of each litho-unit have been mapped together in the lithological map.

TABLE 1 Contingency Table or Confusion Matrix of G-Truths

		PREDICTED CATEGORY									
		Veg-1	Veg-2	Qtz-1	Qtz-2	Phyl	Gran-1	Gran-2	Water	Other	Total Pixel
A	Veg-1	40	0	0	0	0	0	0	0	4	44
C	Veg-2	2	52	0	0	1	3	0	0	3	61
T	Qtz-1	0	1	1584	0	123	6	0	0	78	1792
U	Qtz-2	0	0	0	373	0	17	153	80	34	657
A	Phyl	0	14	113	0	1430	32	0	0	73	1662
L	Gran-1	0	83	1	83	29	1434	9	23	148	1810
	Gran-2	0	0	0	27	0	5	315	7	0	354
C	Water	0	0	0	0	0	0	2	14	0	16
A	Total#	42	150	1698	483	1583	1497	479	124	340	6396
T.	Accu- racy## (%)	95.4	245.9	94.7	73.5	95.2	82.7	135.3	775		

N.B.: ACTUAL CAT. = ACTUAL CATEGORY

(i) Veg-1 = Vegetation-1, Veg-2 = Vegetation-2, Qtz-1= Quartzite-1, Qtz-2 = Quartzite-2, Phyl = Phyllites, Gran-1 = Granite-1, Gran-2 = Granite-2.

(ii) '#' represents the total number of training pixels of actual categories classified as each predicted category; this is obtained by summing up the numbers in each column. For example, the number of training pixels of the various actual categories classified as the predicted category, vegetation-1 is equal to 42.

(iii) '##' represents the percentage by which an actual category is represented on the digital classified image. For any actual category (say Veg-1), this is obtained by dividing the total number of pixels of various actual categories in rows classified as the predicted category, Veg-1 (i.e. the sum of the elements in the column corresponding to the predicted category, Veg-1) by the actual number of training samples extracted for that actual category i.e. Veg-1. For example, for Vegetation-1 class, this may be determined by dividing 42 by 44 and then taking the percentage, that is, $(42/44) \times 100 = 95.4$.

TABLE 2 Confusion Matrix of Training Classes in Percentage

		PREDICTED CATEGORY									
		Veg-1	Veg-2	Qtz-1	Qtz-2	Phyl	Gran-1	Gran-2	Water	Other	Total Pixel
A	Veg-1	90.9	0	0	0	0	0	0	0	9.1	100
C	Veg-2	3.3	85.2	0	0	1.6	4.9	0	0	4.9	100
T.	Qtz-1	0	0.05	88.4	0	6.9	0.33	0	0	4.35	100
	Qtz-2	0	0	0	56.8	0	2.6	23.3	12.2	5.2	100
C	Phyl	0	0.8	6.8	0	86.0	1.9	0	0	4.4	100
A	Gran-1	0	4.6	0.05	4.6	1.6	79.2	0.5	1.3	8.2	100
T.	Gran-2	0	0	0	7.6	0	1.4	90.0	2.0	0	100
	Total#	3.3	5.45	6.85	12.2	10.1	11.13	36.3	15.5		

N.B.: ACT. CAT. = ACTUAL CATEGORY

(i) Veg-1 = Vegetation-1, Veg-2 = Vegetation-2, Qtz-1= Quartzite-1, Qtz-2 = Quartzite-2, Phyl = Phyllites, Gran-1 = Granite-1, Gran-2 = Granite-2.

(ii) '#' represents the total percentage of samples of actual categories misclassified as a predicted category; obtained by summing up the off-diagonal elements in the columns for respective predicted category. For example, the various actual categories misclassified as the predicted category, Granite-2 is obtained by summing up the off-diagonal elements in its column, that is, $23.3 + 0.5 + 12.5 = 36.3$. Granite-2 is the most misrepresented class on the digital thematic image.

CONCLUSION

The study has revealed that the spectral characteristics of the rock types can be studied in a more realistic manner considering the sun-facing and shadowed portions of each unit as separate classes in the classification of digital data. The similar spectral reflectance between different rock types is attributable to the confusing influence of vegetation and identical mineralogical composition. Field reflectance spectra of the different litho-units is essential to supplement the observation made on the thematic image. It is suggested that analysis of thermal infrared reflectance data may be carried out for better discrimination among the litho-units.

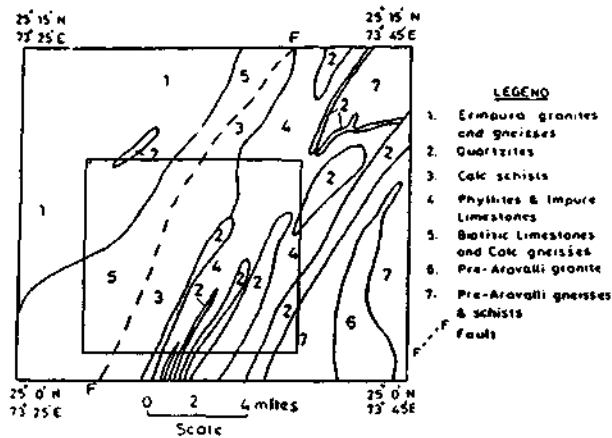


Fig. 1 Geological map of the study area (Modified from Geological Survey of India Memoirs, Vol. 79 Plate 38, 1953). The inner rectangle represents the area covered in the present study.

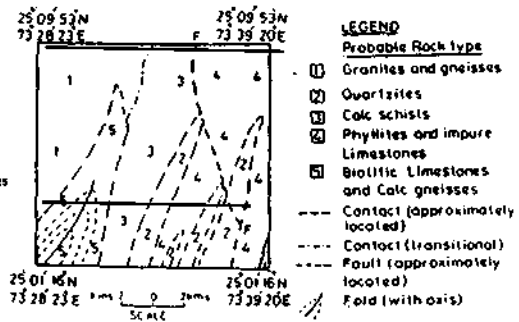


Fig. 3 Geological map of the study area prepared from the digital thematic image.



Fig. 2 Digital thematic image of the study area generated by using maximum likelihood classifier (using TM bands 1, 2, 3, 4, 5, and 7).

REFERENCES

1. D. Evans, Multisensor classification of sedimentary rocks, Remote sensing of environment. 25, 129-144 (1988).
2. L.C. Rowan, C. Anton-Pacheco, D.W. Brickey, M.J. Kingston, A. Payas, N. Vergo and J.K. Crowley, Digital classification of contact metamorphic rocks in Extremadura, Spain using Landsat thematic mapper data, Geophysics. 52, #7, 885-897 (1987).
3. D.B. Segal and I.S. Merin, Successful use of Landsat thematic mapper data for mapping hydrocarbon microseepage induced mineralogic alteration, Lisbon valley, Utah, PE&RS. 55, #8, 1137-1145 (1989).
4. A.M. Heron, The geology of Central Rajputana, Memoirs of the Geological Survey of India. 79 (1953).
5. M.S. Krishnan, Geology of India and Burma, CBS, New Delhi, 1982.